FATIGUE BEHAVIOR OF A DEVELOPED UHPC-FILLED PRECAST DECK JOINT IN BULB-TEE BRIDGE GIRDER SYSTEM REINFORCED WITH SAND-COATED GFRP BARS

Imad Eldin Khalafalla and Khaled Sennah
Civil Engineering Department, Ryerson University, Toronto, Ontario, Canada

Abstract: This paper investigates experimentally the use of corrosion-resistant glass fiber reinforced polymer (GFRP) bars to reinforce the precast deck slab joints in prefabricated bridge bulb-tee (DBT) girders system. In this system the concrete deck slab is cast with a prestressed girder and casting a closure strip between precast flanges to provide continuity between the girders. The aim of this study is to develop joint detail between the precast flanges of the DBT girders, incorporating sand-coated GFRP bars with headed ends embedded in a closure strip filled with ultra-high-performance concrete (UHPC). Two actual-size, GFRP-reinforced, precast concrete deck slabs were erected to perform fatigue tests and determine their behavior under CHBDC truck wheel loading. Each slab has 200 mm thickness, 2500 mm width and 3500 mm length in the direction of traffic. Fatigue behavior and fatigue life of the GFRP reinforced precast (DBT) bridge girders system were investigated using different schemes of cyclic loadings (accelerated variable amplitude cyclic loading as well as constant amplitude cyclic loading followed by loading the slab monotonically to failure). Overall, the test results demonstrated the excellent performance of the developed closure strip details.

1. INTRODUCTION

The use of glass fiber reinforced polymer (GFRP) bars to replace reinforcing steel in deck slabs of precast bulb-tee girders is considered an excellent solution to eliminate the deterioration of deck slabs due to corrosion of steel reinforcement. GFRP is an anisotropic two-component composite material consisting of high strength fibers embedded in a polymer matrix. GFRP reinforcing bars offer advantages over conventional steel reinforcement. These advantages include corrosion resistance, high tensile strength, improved fatigue life, durable and light weight.

A prefabricated bridge system made of deck bulb-tee (DBT) girders, shown in Fig. 1, can be an attractive choice for accelerating bridge construction. In this system, the concrete deck slab is cast with a prestressed girder under controlled conditions at a fabrication facility and then transported to the bridge site. This system requires that longitudinal deck joints be provided to transfer the load between adjacent units. Prefabricated elements, which can be quickly assembled, could reduce design efforts, negative impact on the environment in the vicinity of the site, lane closure times and inconvenience to the traveling public.

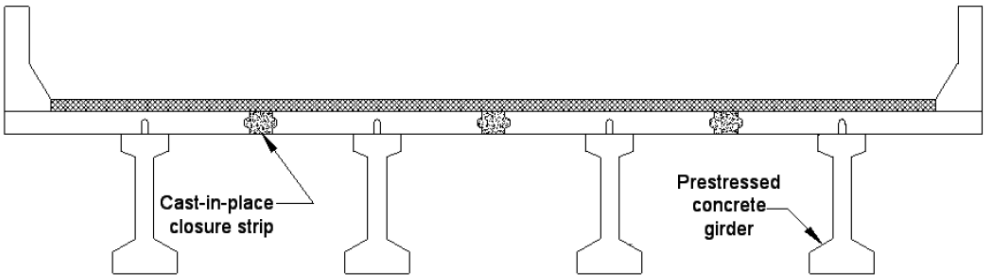

Fig. 1 Prefabricated bridge superstructure made of bulb-tee girders

Development of UHPC-filled precast deck joint in DBT girders system reinforced with GFRP bars not only addresses the corrosion related problem of reinforcing steel bars, but also provides advanced high

performance connection technique for accelerating bridge construction and replacement. This system combines the advantage of the corrosion resistance of GFRP reinforcing bars with the superior properties of the UHPC, such as high strength, increased bond capacity and durability. Because this is a relatively new technology, the Canadian Highway Bridge Design Code, CHBDC, and AASHTO-LRFD Bridge Design Specifications do not provide guidance to design prefabricated concrete girder/deck joints made with GFRP bars. Also, there is not enough information available in the literature to design such joints, nor is there test data available to give confidence to the design of such joints. Most recently, a few authors developed and tested to failure joint details between flanges of precast bulb-tee girders with projecting straight/U-shaped/headed steel bars (among them: Shah et al., 2006, 2007; Au et al., 2008; Li et al., 2010; Au et al., 2011; Graybeal, 2011).

The deck slabs are the part of bridge most prone to repeated moving wheel loads. The design of concrete deck slabs is governed by long-term fatigue endurance and durability of constituent materials. A Literature survey showed that limited number of experiments conducted on bridge deck slabs to examine their fatigue and ultimate load carrying capacity under wheel loads (among them: Sonoda and Horikawa, 1982; Pardikaris and Beim, 1988; Mufti et al., 1993; Matsui et al., 2001; Mufti et al., 2002; Graddy et al., 2002; El-Ragaby et al., 2007). This paper presents an investigation of fatigue behavior of a developed UHPC-filled precast deck joint in DBT girders system reinforced with GFRP bars. Two full-scale bridge deck slab models were built to perform fatigue tests to determine their behavior under CHBDC truck wheel loading. The following sections summarize the specimens' details, test setup, experimental test procedure and test results.

2. DESCRIPTION OF PRECAST BRIDGE DECK SLAB MODEL

Due to the environmental effects and the use of de-icing salts in winter times, many of the North American bridges were severely deteriorated due to corrosion of reinforcing steel and in need of regular maintenance, repair and rehabilitation. Using GFRP-reinforcing bars as internal reinforcement in concrete to replace reinforcing steel in deteriorated deck slabs is a relatively new application. Experimental investigations into the behavior of GFRP-reinforced deck slabs in general are limited, especially those into the fatigue performance (Kumar and GangaRao, 1998; Rahman et al., 2000; Matsui et al., 2001; EL-Gamal et al., 2005; El-Salakawy et al., 2005; Benmokrane et al., 2006; El-Ragaby et al., 2007). Hence, it is necessary to understand the fatigue behavior of such GFRP-reinforced bridge decks, given the new GFRP configurations with the presence of headed stud ends. GFRP bars with headed-end and straight part used in this study have a tensile strength of 1184 MPa and modulus of elasticity of 62.5 GPa. The special sand-coated surface profile of these bars, shown in Fig. 2, ensures optimal bond between the concrete and the bar. The head of 16 mm diameter bar used in this study is approximately 100 mm long, with outer diameter of 50 mm (3.0 times the diameter of the bar) tapers in five steps to the outer diameter of the straight bar. This geometry ensures optimal anchorage forces and minimal transverse splitting action in the vicinity of the head. Given the GFRP's small transverse strength and relatively low modulus of elasticity, the shear strength of GFRP reinforced deck slab is lower than that for steel-reinforced deck slab. However, this issue is not important since shear strength in deck slabs is provided primarily by concrete.

Two full-scale precast bridge deck slab models were designed according to CHBDC specifications were tested in this study. Each slab was formed of two identical precast slab panels 3500x1187.5x200 mm, with a 50-mm deep, 40-mm wide, trapezoidal shape shear key throughout the girders length. The precast slabs represent the flange portions of adjacent bulb-tee precast pretensioned concrete girders shown in Fig. 3(a). A 125-mm wide closure strip was introduced between the precast flanges of the bulb-tee girders as shown in Fig. 3(b). The precast slab bottom GFRP bars projected into the joint with headed end to provide a 100-mm embedment length in the tension zone of the slab thickness, while the top transverse GFRP bars projected into the joint with a 100-mm embedment length in the compression zone of the joint. It is assumed that DBT girders will be aligned to provide 125-mm gap that can be filled using UHPC having a minimum specified strength of 100-MPa. It should be noted that Fig. 3(b) shows projecting GFRP bars from one side of the joint only for clarity and the joint would consist of staggered projecting bars that would allow for ease of assembly in the bridge site.

3. EXPERIMENTAL PROGRAM

The experimental program included two full-scale deck slab specimens of 200 mm thickness, 2500 mm width normal to traffic and 3500 mm length in the direction of traffic. The deck slab was supported over two W610X241 steel beams of span 7000 mm with transverse bracing at their ends to provide lateral restraints to the deck slab as specified in the CHBDC empirical design method. The centre-to-centre spacing of the supporting beams was taken as 2000 mm. The deck slabs and the supporting beams were made fully composite with shear connector pockets and shear studs. The two deck slabs were reinforced with GFRP bars per the reinforcement ratio specified in CHBDC empirical design method. The deck slabs were formed considering the precast deck system shown in Fig. 1 and the precast flange-to-flange connection detail shown in Fig. 3(b). Headed end GFRP bars of 16-mm diameter, spaced at 140-mm c/c, were used as bottom tension reinforcement while the top main and transverse reinforcements were 12-mm GFRP bars spaced at 200-mm c/c. Transverse bottom reinforcement in the tested slabs were provided by 16-mm diameter GFRP bars, spaced at 225-mm c/c. Bottom and top concrete covers of 38 mm were used for the deck slab. Figure 4 illustrates sequence of construction and assembly of the precast jointed slabs.

A ready mix concrete having a specified 28-day compressive strength of 35 MPa was used for precast deck slabs. Standard cylinders of 150-mm diameter and 300-mm height were cast concurrently with the casting of the deck slabs and stored close to the test samples to ensure the same curing conditions after casting. Ultra-High-Performance Concrete (UHPC) having a 28-day specified strength of 100-MPa was used for closure strip. Non-shrink grout extended with 9.5-mm pea gravel was used for shear pockets. The grout has a specified 3-day compressive strength of 31 MPa and 28-day strength of 59 MPa. During the pouring of the UHPC/grout into the precast deck slab closure strips/shear pockets, standard cylinders of 100-mm diameter and 200-mm height were cast and kept close to the test samples. The average compressive strengths of the tested concrete deck slabs S1 and S2 were 57.53 and 44.02 MPa, respectively, while the UHPC average compressive strengths for S1 and S2 were 166.16 and 165.52 MPa, respectively. Table1 summarizes typical field-cast concrete and UHPC material properties.

Fig. 2 Views of GFRP bars

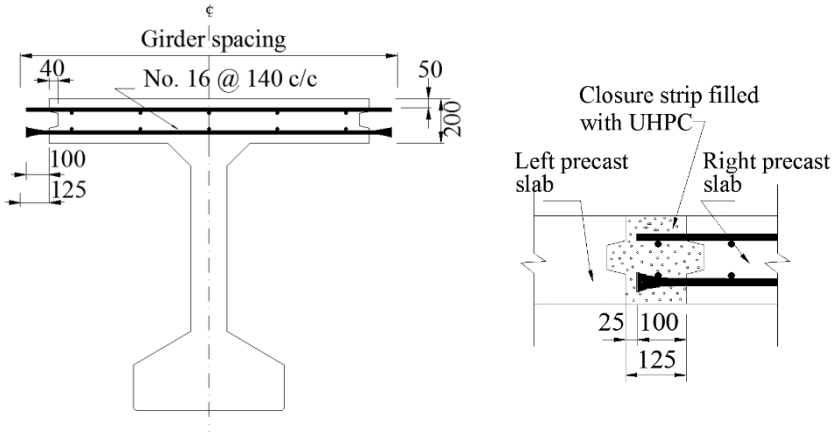

Figure 3 Schematic diagrams of: (a) DBT-girder and GFRP-bars; (b) Proposed closure strip

4. TEST SETUP AND INSTRUMENTATION

All precast slabs were tested under a 250x600 mm single patch load at the center of their clear span. This patch load is equivalent to the foot print of CHBDC wheel load of 87.5 kN. A 50-mm thick steel plate was used to transfer the load to the bridge deck slab; neoprene pad was used to ensure an even distribution of the load pressure on the contact area of the deck slab surface. To apply partial restraint to the slab

ends over the girders, the pair of precast slabs and the supporting girders were made fully composite with shear connector pockets and shear studs. The steel girders were simply-supported over steel pedestals with a clear span of 7000 mm. Elastomeric pads of 300x300x25 mm, were placed between steel pedestals and supporting girders to ensure boundary conditions were achieved. The fatigue load cycles were applied through the use of MTS hydraulic actuator with 500 kN capacity and 250 mm stroke. Figure 5 shows the experimental setup used for testing the deck slab specimens.

The structural response during the cyclic loading or the static loading of the deck slabs was captured through the use of electronic instrumentation. Potentiometers (POTs) and linear variable differential transducers (LVDTs) were used to measure deflections at specified locations of the deck slabs. Electrical-resistance strain gauges were installed on the GFRP bars and the top surface of the deck slab around the loaded area to monitor the strain in the rebar and concrete. Crack displacement transducers were set across the cold joint between the interface of precast panel and the closure-strip to measure the crack width. All instrumentation devices were connected to an electronic data acquisition system (5000) for monitoring and data recording.

Table 1 Typical field-cast concrete and UHPC material properties

Slab	Bar type	Slab type	f_c' (MPa)			Split cylinder cracking strength (MPa)	
			Concrete	UHPC[§]	NSG[*]	Concrete	UHPC[§]
S1	GFRP Sand-coated	Precast with 125 mm closure strip filled with UHPC[§]	57.53	166.16	47.30	3.36	17.70
S2			44.02	165.52	53.96	3.50	19.13

UHPC[§] = ultra-high-performance concrete; NSG[*] = non-shrink grout

5. CYCLIC LOAD TESTS

In this study, two fatigue loading schemes were used, namely: accelerated fatigue loading with variable amplitude fatigue (VAF) loading and constant amplitude fatigue (CAF) loading. Prior to starting fatigue load tests, each slab was pre-cracked by performing static load test up to 1.5 times the fatigue limit state (FLS) loading of 183.75 kN and unloaded to zero. This test was conducted first to determine the cracking load and initiate cracks to simulate real bridge state of stress. In the VAF loading test, the slab was subjected to sinusoidal waveform fatigue load cycles between a minimum load level and variable maximum load levels. The minimum load level was set at about 15 kN, representing the effect of superimposed dead loads on bridge deck (i.e. asphalt and insulation layers). This minimum load level will assist in preventing any impact during cyclic loading. Different peak load levels were selected as multiples of the fatigue limit state (FLS) loading as specified in CHBDC. The CHBDC FLS load is specified using the maximum wheel load of 87.5 kN with 40% dynamic load allowance and a FLS live load factor of 1.0. This leads to a FLS load of 87.5x1.4x1.0 = 122.5 kN, according to CHBDC Clause 3.5.1. In this study, a maximum peak load levels of 1.0, 1.5, 2.0, 2.5, 3.0, 3.5 and 4, which correspond to 122.5, 183.75, 245.00, 306.25, 367.50, 428.75 and 490.00 kN, respectively. Each maximum peak load level was applied for 100,000 cycles at frequencies of 2 Hz or less, depending on the stiffness of the specimen. It should be noted that at the end of each maximum peak load level, a static load test similar to the pre-cracked static load test was conducted to assess the degradation that may occur in the deck slab due to fatigue loadings. This VAF loading was applied to the first deck slab, S1.

A CAF loading test, followed by loading the slab monotonically to failure, was applied for the second deck slab, S2. In this loading test, constant amplitude of load, representing the FLS load specified in CHBDC of 122.5 kN, was applied at a frequency of 4 Hz for 4 million cycles. Similar to the VAF, but at the end of each 250,000 cycles at a specified load level, a static load test was conducted. After completing the cyclic loadings of 4 million cycles, a static load to failure was applied. The static loading was completed through the use of manually operated hydraulic jack and the load was applied in monotonic increments with

temporary holds occurring at approximately 50 kN intervals to allow for inspection of crack initiation and propagation.

(a) Before pouring concrete

(b) After pouring concrete

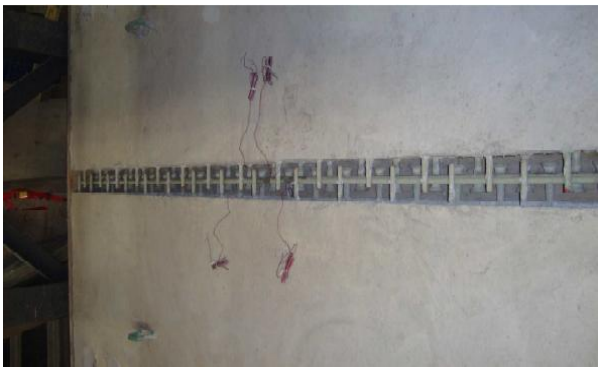

(c) Before pouring UHPC

(d) After pouring UHPC

(e) Before grouting

(f) After grouting

Figure 4 Jointed precast deck slabs fabrication

6. TEST RESULTS

This section discusses the structural behavior of the tested specimens in the form of crack pattern, slab vertical deflection and ultimate load carrying capacity. The first deck slab, S1 was tested under VAF loading. Figure 6 shows the crack pattern at failure on top and underside of the precast deck slab S1. During the pre-cracking test for the deck slab, it was observed that first hairline cracks formed at the cold

joint between the precast concrete and the closure strip at 47 kN and the maximum measured crack width at service load level was 0.11 mm. After starting the cyclic loading, these fine cracks started to widen gradually and propagated deeper, and new transverse cracks developed at mid-span under the loaded area. With increasing load cycles, more cracks developed in the longitudinal and radial directions. After completing 100,000 cycles at a fatigue load range of 367.5kN, a transverse crack was observed across the closure strip at mid-span under the loaded area. After that the deck slab started to undergo drastic decrease in flexural stiffness and the remaining peak loads were applied with reduced frequencies. It should be noted that the maximum fatigue load range reached at the final peak load level was 475 kN at a frequency of 0.5 Hz. The jointed deck slab,S1 failed under punching shear at a fatigue load range of 475 kN and after completing 886,346 cycles.

(a) Fatigue load test

(b) Static load test

Figure 5 Views of test setup

Figure 8(a) shows the static load-deflection relationships of slab S1 after different variable amplitude fatigue (VAF) loading steps. In Fig. 8(a) the term “S” refers to the static loading following the completion of each fatigue loading step, while the number following “S-” refers to the fatigue load at which the slab completed 100,000 load cycles. For example, S-122.5 kN refers to the static loading and unloading cycle after completing 100,000 cycles at a fatigue load range of 122.5 kN. It can be observed that with the increase in the peak load and number of cycles, a progressive loss of flexural stiffness and increase in both vertical and residual deflection occurred in the deck slab. Figure 8(a) also indicates that the deck slab, S1, exhibited linear load-deflection relationships up to a fatigue load range of 428.75 kN and 600,000 load cycles.

The second deck slab, S2 was tested under CAF loading. Figure 7 shows the crack pattern at failure on top and underside of deck slab, S2. Before starting the pre-cracking test, there were few cracks at the underside of the deck slab in the longitudinal and transverse directions. These cracks occurred during

transportation of the slab specimen and the maximum measured width of these cracks was 0.175 mm. During the pre-cracking test for the deck slab, it was observed that first hairline cracks formed at the cold joint between the precast concrete and the closure strip. After the pre-cracking test, the deck slab was subjected to 4,000,000 cycles at a fatigue load range of 122.5 kN and a frequency of 4 Hz. After completing the cyclic load, a static test was applied until failure. The deck slab failed at a maximum load of 801.6 kN and a maximum deflection of 24.41 mm. The failure was due to punching shear as shown in Fig. 7. CHBDC specifies truck wheel load of 87.5 kN, load factor of 1.7 and dynamic load allowance of 0.40 for the design of deck slabs. This makes the factored applied design wheel load 208.25 kN. Since the experimental ultimate load of the pre-fatigued slab is 801.6 kN, one may conclude that the experimental ultimate load is more than three times the factored load specified by CHBDC.

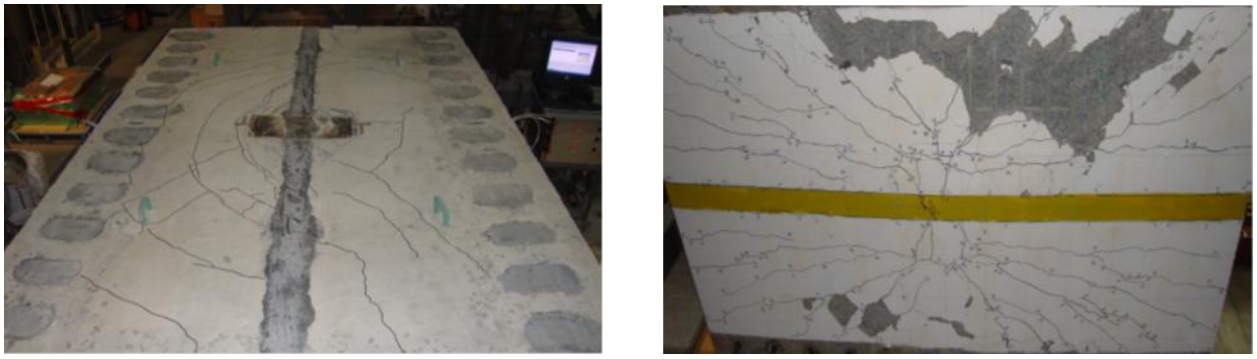

(a) Top surface (b) Bottom surface

Figure 6 Views of punching shear crack pattern and failure of precast jointed slab S1

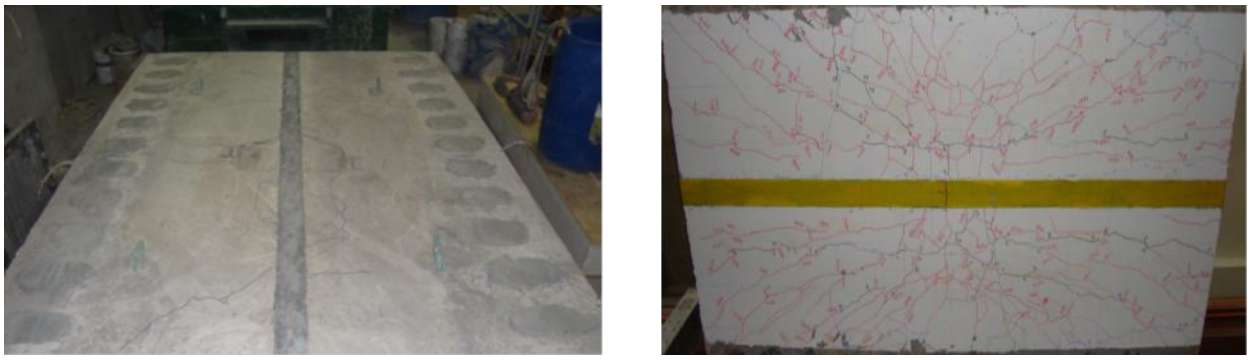

(a) Top surface (b) Bottom surface

Figure 7 Views of punching shear crack pattern and failure of precast jointed slab S2

Figure 8(b) shows the static load-deflection relationships of slab S2 after different constant amplitude fatigue (CAF) loading steps. It should be noted that the term “S” in Fig. 8(b) refers to the static loading following the completion of each fatigue loading step, while the number following “S-” refers to the number of completed load cycles. For example, S-250,000 refers to static loading and unloading cycle after completing 250,000 cycles. It is obvious that slab S2 exhibited linear behavior with almost similar slopes of the load-deflection relationships after being subjected to 4,000,000 load cycles at a fatigue load range of 122.5 kN. This indicates that there was no reduction in the slab flexural stiffness during the CAF test. One can conclude that GFRP-reinforced slab showed high fatigue performance and there was no observed fatigue damage when subjected to 4,000,000 load cycles under FLS load range of 122.5 kN specified in the CHBDC.

Figure 9 depicts the static load-maximum deflection relationship obtained at mid-span of the pre-fatigued deck slab S2. It can be observed that the deck slab exhibited linear deflection behaviour up to approximately 240 kN. This load exceeds CHBDC factored design load of 208.25 kN by about 16% before undergoing a change in slope as the flexural stiffness gradually decreased. After this load, deck slab S2 exhibited a bit linear behaviour up to failure. Given the linear nature of the load-deflection relationship from the cracking load to failure, the recorded punching shear failure of the tested deck slab was sudden. Also, it can be noticed that the maximum measured vertical deflection at service load of 110.25 kN was 1.1 mm, which is less than the allowable limit specified by AASHTO-LRFD specifications, (L/800=2.5 mm, where L is the slab span of 2000 mm).

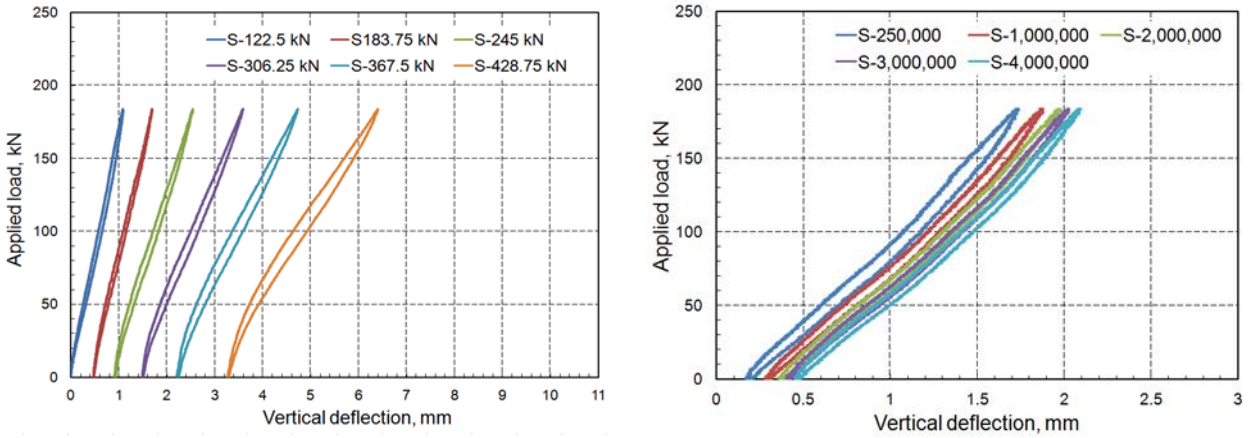

(a) S1: loaded with VAF loading (b) S2: loaded with CAF loading

Figure 8 Static load-deflection relationships of slabs S1 and S2 after different fatigue loading steps

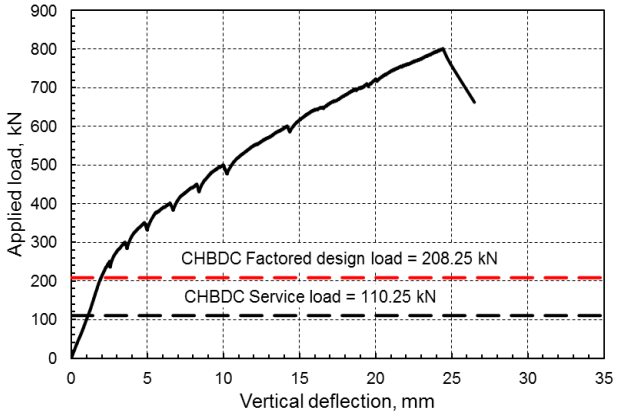

Figure 9 Static load-maximum deflection relationship obtained at mid-span of slab S2

Both deck slabs failed in a punching shear mode at extremely high load capacities. From Figs. 6 and 7, it is clear that the perimeter of punching shear failure did not follow the traditional pattern of being along the perimeter of the 250x600 mm loaded area and a large circle at the underside of the deck slab. Due to the presence of the stiff UHPC in the closure strip, the punching shear cracks at the top surface deviated to the longitudinal direction of the joint rather than crossing the joint. This made the punching shear perimeter at the bottom of the slab to appear close to the supporting steel girders without being connected across the UHPC-filled joint. Also, it can be observed that in case of variable amplitude fatigue (VAF) loading until failure, more cracks were developed on the top surface of the deck slab in addition to the falling of concrete from the bottom surface of the slab compared to the pre-fatigued and monotonically loaded slab.

To determine the punching shear perimeter of the tested deck slabs, the two deck slabs were cut into half along the transverse direction, as shown in Fig. 10, and then one of the halves was cut into half again along the longitudinal direction. From the saw-cut slabs, the widths of the punched sections at the mid-depth of the slabs were measured and the punching shear perimeter was calculated. The average observed mid-depth punching perimeter for the precast jointed deck slabs was measured to be 1.33d away from the sides of the loaded area, which is more than twice the corresponding distance specified in ACI 440.1R-06 and CSA S806-12 for calculating theoretical punching shear perimeter.

Figure 10 Views of saw-cut slab segments after punching shear failure for deck slabs S1and S2

7. CONCLUSIONS

This paper investigates the fatigue behavior and fatigue life of a developed UHPC-filled precast deck joint in DBT girders system reinforced with GFRP bars when subjected to CHBDC wheel loading. Based on the experimental results, the following conclusions can be drawn:

1- GFRP-reinforced deck slab showed high fatigue performance and there was no observed fatigue damage when subjected to 4,000,000 cycles under FLS load range of 122.5 kN specified in CHBDC.

2- The ultimate load capacities of the pre-fatigued GFRP-reinforced precast deck slab with a 125-mm wide closure strip and projecting headed-end bars filled with UHPC is more than three times the design factored load of 208.25 kN specified by CHBDC.

3- Under static and fatigue loadings, punching shear is the mode of failure for all tested GFRP-reinforced restrained deck slabs, as expected.

4- GFRP reinforcement ratio specified by CHBDC is adequate to meet the ultimate limit state and fatigue limit state requirements for concrete bridge deck slabs.

5- The average observed mid-depth punching perimeter for the precast jointed deck slab was measured to be 1.33d away from the sides of the loaded area, which is more than twice the corresponding distance specified in ACI 440.1R-06 and CSA S806-12 for calculating theoretical punching shear perimeter.

8. ACKNOWLEDGMENTS

The authors would like to acknowledge the support of Ontario Centers of Excellence's Collaborative Research fund, Pultrall Inc. and Trancels-Pultrall Inc. The authors would also like to thank Euclid Chemical Company for supplying grout material and Lafarge North America Inc. for supplying the UHPC mix.

9. REFERENCES

AASHTO.2010. AASHTO-LRFD Bridge Design Specifications. American Association of State Highway and Transportation Officials. Washington, D.C.

ACI Committee 440. 2006. Guide for the Design and Construction of Structural Concrete Reinforced with FRP Bars, ACI 440.1R-06.American Concrete Institute, Farmington Hills, MI, USA.

Au, A., Lam, C., and Tharmabala, B. 2008.Investigation of Prefabricated Bridge Systems using Reduced-

Scale Models. PCI Journal, 53(6): 67-95.
Au, A., Lam, C., and Tharmabala, B. 2011.Investigation of Closure Strip Details for Connecting Prefabricated Deck Systems. PCI Journal, 56(3): 75-93.
Benmokrane, B., El-Salakawy, E., El-Ragaby, A., and Lackey, T. 2006. Designing and Testing of Concrete Bridge Decks Reinforced with Glass FRP Bars. Journal of Bridge Engineering, ASCE, 11(2): 217–229.
CHBDC.2006. Canadian Highway Bridge Design Code, CSA-S6-06.Canadian Standard Association (CSA), Toronto, Ontario, Canada, 734 pp.
CAN/CSA-S806-12. 2012. Design and Construction of Building Structures with Fibre-Reinforced Polymers. Rexdale, Ontario, Canada, 37pp.
El-Gamal, S., El-Salakawy, E., and Benmokrane, B. 2005. Behavior of Concrete Bridge Deck Slabs Reinforced with Fiber-Reinforced Polymer Bars under Concentrated Loads. ACI Structural Journal, 102(5): 727-735.
El-Ragaby, A., El-Salakawy, E., and Benmokrane, B. 2007. Fatigue Life Evaluation of Concrete Bridge Deck Slabs Reinforced with Glass FRP Composite Bars. Journal of Composites for Construction, 11(3): 258-268.
El-Salakawy, E., Benmokrane, B., El-Ragaby, A., and Nadeau, D. 2005. Field Investigation on the First Bridge Deck Slab Reinforced with Glass FRP Bars Constructed in Canada. Journal of Composites for Construction, 9(6): 470-479.
Graddy, J., Kim, J., Whitt, J., Burns, N. and Klingner, R. 2002.Punching Shear Behavior of Bridge Decks under Fatigue Loading. ACI Structural Journal, 90(3): 257-266.
Graybeal, B.2011. Fatigue Response in Bridge Deck Connection Composed of Field-Cast Ultra-High-Performance Concrete. Journal of the Transportation Research Board, No. 2251, Transportation Research Board of the National Academies, Washington, D.C., pp. 93-100.
Kumar, S. and GangaRao, H. 1998. Fatigue Response of Concrete Decks Reinforced with FRP Rebars. Journal of Structural Engineering, 124(1): 11-16.
Li, L., Ma, Z., Griffey M.E. and Oesterle, R.G. 2010. Improved Longitudinal Joint Details in Decked Bulb Tees for Accelerated Bridge Construction: Concept Development, Journal of Bridge Engineering, ASCE, 15(3): 327–336.
Matsui, S., Tokai, D., Higashiyama, H. and Mizukoshi, M. 2001. Fatigue Durability of Fibre-Reinforced Concrete Decks Under Running Wheel Load. Proceedings of the 3rd International Conference on Concrete Under Severe Conditions, University of British Columbia, Vancouver, Canada, pp 982-991.
Mufti, A., Jaeger, L., Bakht, B., and Wegner, L. 1993. Experimental Investigation of FRC Slabs without Internal Steel Reinforcement. Canadian Journal of Civil Engineering, 20(3): 398-406.
Mufti, A., Memon, A., Bakht, B., and Banthia, N. 2002. Fatigue Investigation of the Steel-Free Bridge Deck Slab. ACI International SP-206, American Concrete Institute, Farmington, Hills, Michigan, USA: 61-70.
Perdikaris, P., and Beim, S. 1988. RC Bridge Decks under Pulsating and Moving Load. Journal of Structural Engineering, 114(3): 591-607.
Rahman, A., Kingsly, C., and Kobayashi, K. 2000. Service and Ultimate Load Behavior of Bridge Deck Reinforced with Carbon FRP Grid. Journal of Composites for Construction, 4(1): 16-23.
Shah, B., Sennah, K., Kianoush, R., Tu, S. and Lam, C. 2006.Flange-to-Flange Moment Connections for Precast Concrete Deck Bulb-Tee Bridge Girders. Journal of Prestressed Concrete Institute, PCI, 51(6): 86-107.
Shah, B., Sennah, K., Kianoush, R., Tu, S. and Lam, C. 2007.Experimental Study on Prefabricated Concrete Bridge Girder-to-Girder Intermittent-Bolted Connection Systems. ASCE journal of Bridge Engineering, 12(5): 570-584.
Sonoda, K., and Horikawa, T. 1982. Fatigue Strength of Reinforced Concrete Slabs under Moving Loads. Proceedings of the IABSE Colloquium on Fatigue of Steel and Concrete Structures, International Association for Bridges and Structural Engineering, Zurich, Switzerland: 455-462.